Structures and dynamical properties of C_n, Si_n, Ge_n, and Sn_n clusters with n up to 13

Zhong-Yi Lu, Cai-Zhuang Wang, and Kai-Ming Ho
Ames Laboratory–U.S. Department of Energy and Department of Physics and Astronomy, Iowa State University, Ames, Iowa 50011
(Received 12 July 1999)

Car-Parrinello molecular dynamics simulated annealings were carried out for clusters Si_n, Ge_n, and Sn_n ($n \leqslant 13$). We investigate the temperature regions in which these clusters transform from a ''liquidlike'' phase to a ''solidlike'' phase, and then from the ''solidlike'' phase to the ground-state structures. Additional simulated annealing was also performed for the cluster C_{13} which is selected as a prototype of small carbon clusters. In addition to the discovery of structures for Sn and Ge clusters, our simulation results also provide insights into the dynamics of cluster formation.

I. INTRODUCTION

Atomic clusters of semiconductor elements are of great interest and importance from both academical and technological point of view. Cluster is an intermediate phase between single atom and bulk materials. It has been shown that, for example, small Si clusters are not simple fragments of bulk tetrahedral lattices.[1] A fundamental issue is to understand how the atomic and electronic structures and properties of the clusters change with its aggregation size increasing from single atom to bulk materials.

Over the past decade, semiconductor clusters, especially carbon and Si clusters, have been a subject of intensive studies.[1–5] The atomic structures of Si_n and Ge_n have been studied in detail for $n \leqslant 10$ (n denotes the number of atoms in the clusters).[5] Very recently, knowledge of Si_n structures is extended to the medium-size $n = 11-20$.[6] For Sn_n clusters, it was shown that the structures are similar to those of the corresponding Si and Ge clusters for $n \leqslant 7$.[7] C_n clusters are well studied.[2,3] Their structures adopt either linear chains or monocyclic rings for $n \leqslant 19$, and fullerene structures for $n \geqslant 24$.[8]

In contrast to the progress in the structure determination, the dynamics of the cluster formation is much less understood. Recently, we have systematically carried out plane-wave Car-Parrinello (CP) *ab initio* molecular dynamics (MD) (Ref. 9) simulated annealings for Si_n, Ge_n, and Sn_n clusters with n up to 13.[10] Additionally, we have also performed such simulations for C_{13} which was selected as a prototype for small C clusters. In this paper, these simulation results are analyzed in order to gain some insights into the dynamics of cluster formation. New structures found for Sn and Ge clusters are also reported.

II. SIMULATION TECHNIQUES

CP MD is an efficient scheme to perform *ab initio* molecular dynamics simulations using the density functional theory within the local density approximation (LDA).[11] CP MD simulations had been successfully applied to many systems including melting of bulk Si,[12] incomplete melting on Si(111) surfaces[13] and Ge(111) surfaces,[14] and dynamical properties of liquid Si and Ge.[15,16] The method has also been shown to work well in searching for the ground state structures of small Si_n clusters ($n < 10$).[4] In the present CP MD simulations, we used the Ceperley-Alder exchange-correlation potential functional with the parametrization of Perdew and Zunger.[17] The electron-ion interaction is represented by *ab initio* norm-conserving pseudopotential[18] in the Kleinman-Bylander form.[19] Specifically, for C a Car-von Barth atomic pseudopotential[3] was used with s nonlocality. For Si, Ge, and Sn, we used the pseudopotentials with s and p nonlocality.[20] The Kohn-Sham orbitals were expanded in a plane-wave basis set with an energy cutoff of 35 Ryd for C and 10 Ryd for Si, Ge, and Sn. Only the Γ point was used in the sampling of electronic structures since a large supercell was used in the simulation.

The Verlet algorithm was used to integrate the equations of motion. With the ''preconditioned'' method,[21] we were able to increase the integration time step to 6 a.u. for C and 15 a.u. for Si, Ge, and Sn with the fictitious electronic mass of 260 a.u. We used two separate Nosé thermostats for the ionic and electronic subsystems, respectively,[22] when the simulated clusters become metallic at high temperatures in order to keep the system on the Born-Oppenheimer surface. The electronic Nosé frequency was set to 100 THz while the ionic Nosé frequency was set to 20 THz for Si, Ge, and Sn, but 50 THz for C, in accordance with their bulk maximum phonon frequencies.[23]

In our simulations, the starting atomic configurations were set up by random selections of atomic positions with a constraint that the separation of any pair of atoms is not less than the bulk bond length and all atoms are confined in a small cubic cell chosen such that its atomic density is roughly equal to that of the bulk. The small cubic cell is embedded in a large cubic supercell with edge equal to 35 a.u., and periodic boundary conditions were imposed on the large cubic supercell. The size of the periodic supercell is large enough to decouple the artificial interaction between the clusters. For example, for Si_n, Ge_n, and Sn_n with n up to 30, the supercell would be expected to have more than 10 Å vacuum region since Si, Ge, and Sn clusters would adopt compact structures. Although C_{13} could take a linear chain structure in the annealing process, the chain length is estimated to be less than 28 a.u. Thus, even for C_{13}, we will not have problems with a supercell of 35 a.u. in each dimension.

In our simulations, Si, Ge, and Sn clusters were quickly heated to 3000, 2400, and 1980 K, respectively, in 3000 MD

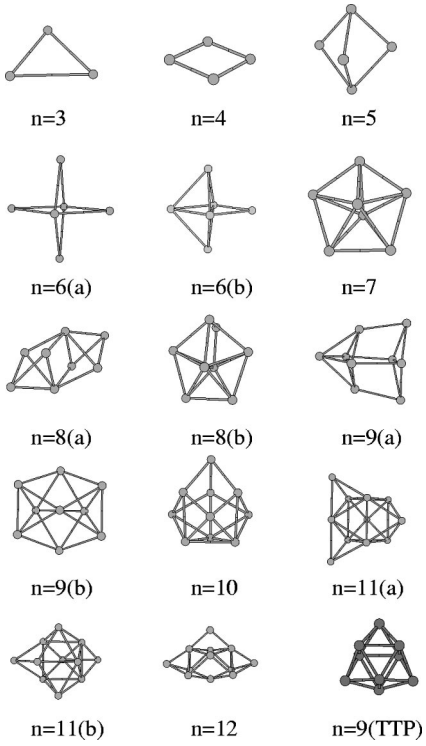

FIG. 1. Structures of Si_n, Ge_n, and Sn_n ($n=3-12$). For $n\leqslant 7$ and $n=10$, 12, Si_n, Ge_n, and Sn_n share the similar structures. Note the structure of $n=6(a)$ is obtained by our simulation, which is energetically degenerate with that of $n=6(b)$ previously proposed (Ref. 1). For $n=8$ and 9, Si_n and Ge_n adopt 8(a) and 9(a) while Sn_n adopt 8(b) and 9(b), respectively. For $n=11$, Si_n adopts 11(a) while Ge_n and Sn_n adopt 11(b). The corresponding cohesive energies and energy-gaps between HOMO-LUMO are summarized in Table I.

steps (about 1.1 ps), followed by another 3000 MD steps at these temperatures to enforce them sufficiently in equilibrium. After that, the hot clusters were cooled down very slowly and uniformly to zero temperature in 60 000 MD steps (about 22 ps). The cooling rates were 5, 4, and 3.3 K per 100 MD steps for Si, Ge, and Sn, respectively.

The above simulated annealing procedure results in ground state structures for Si_n, Ge_n, and Sn_n clusters up to $n=13$.[10] We verify this by comparing with structures obtained from previous studies (e.g., those in Refs. 1, 4, and 5). We also cross checked our results by exchanging the structures of the Si, Ge, and Sn clusters of the same size obtained from the above simulated annealings, with a proper scaling (1:1.06:1.22 for Si:Ge:Sn) and relaxation. The clusters obtained from simulated annealing were reheated up to 800, 600, and 400 K for Si, Ge, and Sn clusters, respectively, for another 4500 MD steps. All clusters are found to be stable under these temperatures within the simulation time.

In order to examine the dependence of cluster structures and dynamics on the simulated annealing conditions, we have performed another three independent simulated annealings for Si_{13} with different starting configurations. The first two annealings were from 3300 and 3000 K, and with 10 and 12 Ryd as the energy cutoff, respectively. The third was from 2500 K and with 10 Ryd as the energy cutoff, but the cooling rate was reduced to 3.125 K per 100 MD steps.[24] In the end all these annealings for Si_{13} led to the same structure shown in Fig. 2, which has C_s symmetry and is 19 meV/

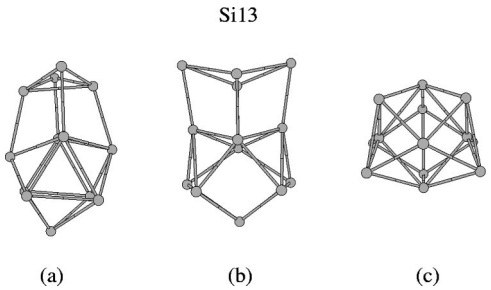

FIG. 2. Final structure by the simulated annealing for Si_{13}: (a) Side view; (b) other side view; and (c) top view. The corresponding cohesive energy and energy-gap between HOMO-LUMO are reported in Table I.

atom lower in energy than the C_{3v} isomer obtained in previous Car-Parrinello simulations.[25] We perform one more simulation starting from the C_{3v} structure. After running 6000 MD steps at 3000 K, the cluster is gradually cooled to zero temperature. We again reached the C_s structure as obtained from the random starting configurations. With all these calculations, we are confident that we have located the global minima.

III. ANALYSIS AND RESULTS

We show the cluster structures obtained from our simulations in Figs. 1, 2, 3, and 4. The corresponding cohesive energies and energy gaps between the highest occupied molecular orbit (HOMO) and lowest unoccupied molecular orbit (LUMO) are summarized in Table I. Our structures for Si_n ($n\leqslant 10$) agree with the previously accepted ones.[1,4,5] Our results show that Ge_n and Sn_n ($n\leqslant 12$) share similar structures as Si_n except for Sn_8, Sn_9, Sn_{11}, and Ge_{11}. The structure of Sn_8 obtained from our simulated annealing is a pentagonal bipyramid with one atom added to it [Fig. 1 $n=8(b)$]. The structures of Sn_9 consists of two tetragonal bipyramids [Fig. 1 $n=9(b)$], and that of Sn_{11} is a pentacapped trigonal prism [Fig. 1 $n=11(b)$]. The structure of Ge_{11} from our simulation as shown in Fig. 1 $n=11(b)$ is similar to that of Sn_{11}. Nevertheless, as one sees from Table I, other isomers of Sn_8, Sn_9, and Sn_{11} obtained by scaling the ground state structures of Ge_8, Ge_9, and Si_{11} have energies very close to those of the ground state isomers. This suggests that Si_n, Ge_n, and Sn_n are very similar for clusters up to $n=12$.

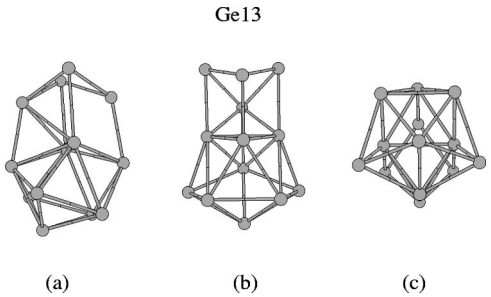

FIG. 3. Final structure by the simulated annealing for Ge_{13}: (a) Side view; (b) other side view; and (c) top view. The corresponding cohesive energy and energy-gap between HOMO-LUMO are reported in Table I.

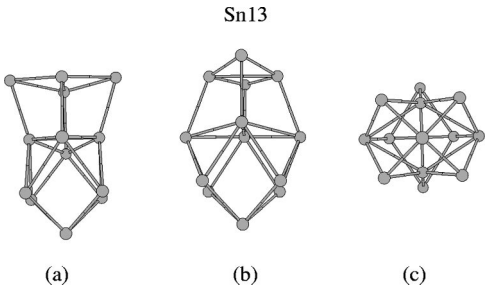

FIG. 4. Final structure by the simulated annealing for Sn_{13}: (a) Side view; (b) other side view; and (c) top view. Note that when Ge_{13} adopts this structure, it is degenerate in energy with that one shown in Fig. 3. The corresponding cohesive energy and energy-gap between HOMO-LUMO are reported in Table I.

For Si_{13} and Ge_{13}, the lowest energy structures obtained from the simulated annealings differ with each other even though both has a C_s symmetry (Figs. 2 and 3). The ground state structure of Sn_{13} (Fig. 4) has C_{2v} symmetry. This C_{2v} structure, if adopted by Ge_{13}, will have an energy degenerate (within the accuracy of our calculations) to that of the structure obtained from the simulated annealing (see Table I). From Figs. 1, 2, 3, and 4 we see that for $n>9$ the clusters Si_n, Ge_n, and Sn_n all contain a similar structural motif in the form of tricapped trigonal prisms (TTP) cluster with 9 atoms [shown in Fig. 1 $n=9$(TTP)]. In previous work,[6] it has been demonstrated that this structural motif dominates the structures of Si clusters in the range $n=10$–20 before the well-known ''prolate-to-spherical'' structural transition.[26] Our present simulated annealing results suggest that this structural motif is also applicable for Ge and Sn clusters in the same range.

TABLE I. Symmetries (sym), calculated cohesive energies [31] E_c (eV/atom) and HOMO-LUMO energy gap E_g (eV) for the clusters Si_n, Ge_n, and Sn_n ranging from $n=3$–13, which corresponding geometries are shown in Figs. 1, 2, 3, and 4. Note ''13(Si),'' ''13(Ge),'' and ''Sn(13)'' indicate their structures correspond to the ones obtained from the simulated annealings for Si_{13}, Ge_{13}, and Sn_{13}, respectively.

Size	Sym.	E_c [Si]	E_g [Si]	E_c [Ge]	E_g [Ge]	E_c [Sn]	E_g [Sn]
3	C_{2v}	2.924	1.00	2.659	1.38	2.227	1.10
4	D_{2h}	3.504	1.06	3.187	1.15	2.736	0.98
5	D_{3h}	3.786	1.97	3.452	1.93	2.965	1.25
6(a)	D_{4h}	3.996	2.06	3.636	2.03	3.167	1.56
6(b)	C_{2v}	3.995	2.07	3.634	2.07	3.163	1.63
7	D_{5h}	4.142	2.10	3.769	1.94	3.308	1.55
8(a)	C_{2h}	4.085	1.44	3.685	1.27	3.227	0.88
8(b)	C_s	4.011	0.84	3.681	1.11	3.236	0.88
9(a)	C_{2v}	4.197	1.96	3.791	1.74	3.334	1.36
9(b)	C_{2v}	4.140	1.54	3.782	1.71	3.339	1.34
10	C_{3v}	4.325	2.12	3.907	2.02	3.432	1.54
11(a)	C_{2v}	4.265	1.75	3.809	1.35	3.367	1.12
11(b)	C_s	4.264	1.16	3.838	1.26	3.382	0.94
12	C_{2v}	4.298	2.18	3.855	2.10	3.397	1.75
13(Si)	C_s	4.298	1.02	3.843	1.02	3.387	0.70
13(Ge)	C_s	4.284	1.03	3.856	1.16	3.393	0.84
13(Sn)	C_{2v}	4.261	0.78	3.857	1.16	3.407	0.80

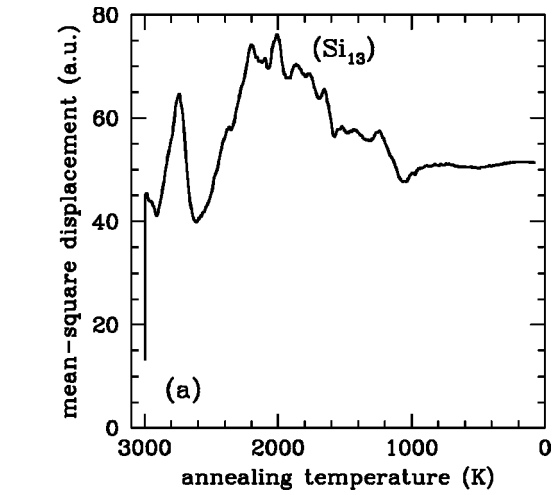

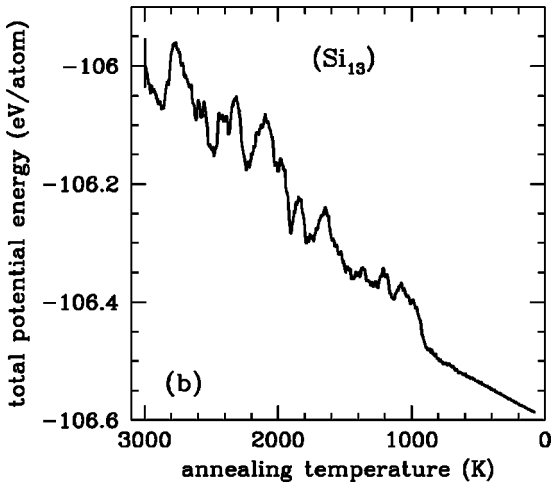

FIG. 5. Si_{13}: (a) mean square displacement vs annealing temperature, (b) total potential energy vs annealing temperature, as obtained by the simulated annealing which started from 3000 K and ran with the cooling rate of 5 K per 100 MD step. An average over every 600 MD steps had been taken to filter out high thermal frequency components. 3000 MD steps are roughly equal to 1.1 ps.

In order to gain some insights into the dynamics of the cluster formation process, we select Si_n with $n=7$ and 13 as the prototypes for further analysis. For Si_{13}, the simulated annealing process with the starting temperature of 3000 K and cooling rate of 5 K per 100 MD steps is displayed in Fig. 5. Every data point in this plot represents an average result over an interval of 600 MD steps in order to filter out high frequency components due to thermal motion. From Fig. 5(a) we see that the mean-square displacement (MSD) begins to become flat around the temperature 2000 K. Above 2000 K the MSD of Si_{13} has drastic changes and fluctuations. Since the simulated clusters are not extended systems, we cannot simply relate the MSD to diffusion coefficient. Nevertheless, the drastic change of MSD with time indicates that the cluster is not in a stable phase. Even though there are some peaks and valleys above 2000 K in Fig. 5(a), they are too narrow to

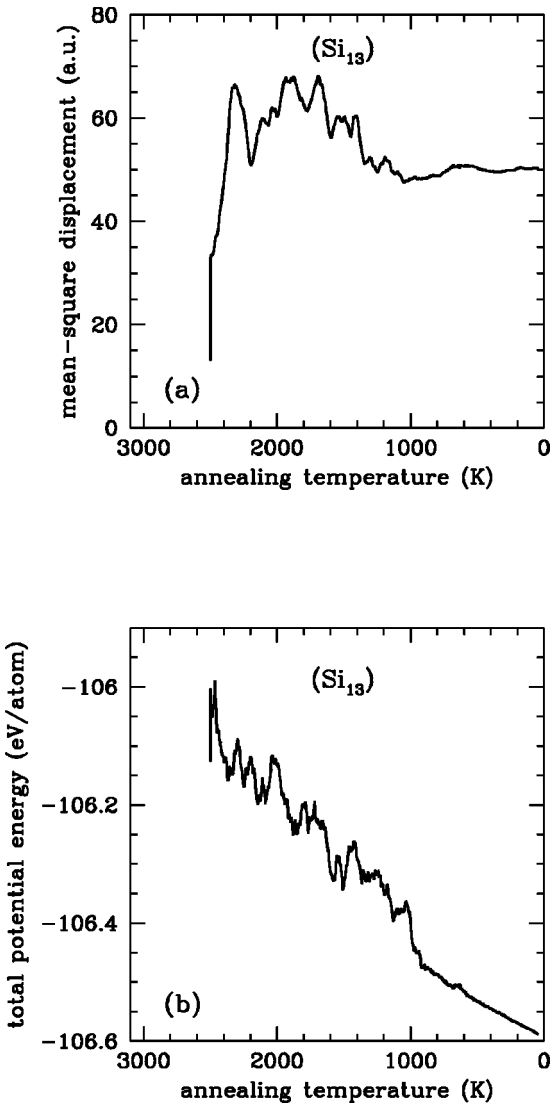

FIG. 6. Si_{13}: (a) mean square displacement vs annealing temperature, (b) total potential energy vs annealing temperature, as obtained by the simulated annealing which started from 2500 K and ran with the cooling rate of 3.125 K per 100 MD step. An average over every 600 MD steps had been taken to filter out high thermal frequency components. 3000 MD steps are roughly equal to 1.1 ps.

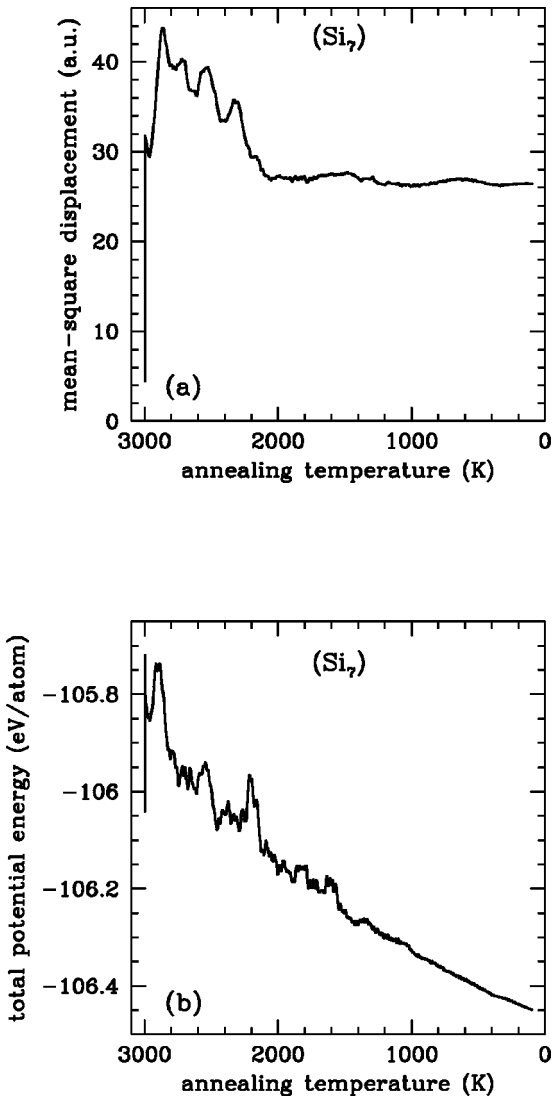

FIG. 7. Si_7: (a) mean square displacement vs annealing temperature, (b) total potential energy vs annealing temperature, as obtained by the simulated annealing which started from 3000 K and ran with the cooling rate of 5 K per 100 MD step. An average over every 600 MD steps had been taken to filter out high thermal frequency components. 3000 MD steps are roughly equal to 1.1 ps.

be considered as signals of meaningful metastable phases. An inspection of the animation of the simulation shows that above 2000 K the Si_{13} sometimes dissociates into fragments mostly contain 4, 6, 7, 1, 3, or 5 atoms. Those peaks or valleys in the MSD above 2000 K are mostly correlated with these dynamical dissociations. In our discussion, the phase in which the MSD of the clusters changes dramatically with time is labeled as the ''liquidlike'' phase. On the contrary, the ''solidlike'' phase indicates that the cluster is in a metastable or stable phase with a flat time-independent MSD. In this language, Si_{13} is in a ''liquidlike'' phase above 2000 K, and takes a transition from ''liquidlike'' phase to ''solidlike'' phase around $T_1 = 2000$ K. Figure 5(a) also shows that the last big jump takes place around $T_2 = 1100$ K. This jump indicates a transition from a metastable ''solidlike'' phase to the stable ''solidlike'' phase which leads to the ground-state structure at zero temperature. Here we call the last stable phase ''ground-state'' phase. The above transition feature is also clearly reflected in Fig. 5(b). In particular, the total potential energy of the cluster decreases linearly with the annealing temperature after 1100 K, which indicates the stable phase has been reached by Si_{13}. Between the transition temperatures T_1 and T_2 there is another drastic transformation around 1600 K. Figure 6 displays another simulated annealing done for Si_{13}, where the starting temperature is 2500 K and the cooling rate is 3.125 K per 100 MD steps. As we see from Fig. 6, Si_{13} again experienced similar jumps around 2000, 1100, and also 1600 K. In this simulation, an additional minor transition was observed around 1300 K. Both Fig. 5 and Fig. 6 show a similar behavior regarding the transition from ''liquidlike'' phase to ''solidlike'' phase and the jump to the ''ground-state'' phase. Similar formation dynamics is also observed in the other simulations of Si_{13} with different simulation conditions as discussed above. We may thus infer that the transition behavior of Si_{13} is intrinsic.

For smaller clusters, there are fewer low-energy isomers,

TABLE II. Temperatures T_1 and T_2 at which the simulated clusters Si_n, Ge_n, and Sn_n ($n=4$ to 13) take the transition from a ''liquidlike'' phase to a ''solidlike'' phase and jump to the ''ground-state'' phase, respectively. The unit in temperature is K.

Size	T_1 [Si]	T_2 [Si]	T_1 [Ge]	T_2 [Ge]	T_1 [Sn]	T_2 [Sn]
4	2400	2400	2000	2000	1800	1800
5	2400	1700	2000	1400	1700	1100
6	2400	2400	2000	2000	1800	1800
7	2200	2200	1900	1900	1600	1600
8	2100	1700	1900	1400	1600	1400
9	1800	1300	1800	1300	1700	900
10	2000	1500	1900	1300	1500	1100
11	2000	1400	1700	1000	1500	1000
12	1900	1300	1600	1000	1500	900
13	2000	1100	1600	1000	1400	900

thus, the formation dynamics of Si_7 is much simpler than that of Si_{13}. The simulated annealing of Si_7 is displayed in Fig. 7. We see that Si_7 directly jumped from the ''liquidlike'' phase to the ''ground-state'' phase, namely, pentagonal bipyramid structure formed already around 2200 K. Formation dynamics of Si_4 and Si_6 also have a simple behavior, similar to that of Si_7. The ground structure phases of Si_4, Si_6, and Si_7 can be maintained at much higher temperatures. This simple formation dynamics may give us a clue for understanding medium-sized Si cluster dissociation process where Si_4, Si_6, and Si_7 are the most popular fragments.[27]

Our simulation results also show that Ge_n and Sn_n exhibit formation dynamics similar to that of Si_n clusters apart from a scaling in temperatures. These results are summarized in Table II. From Table II it is also noted that the transition temperatures T_1, at which the clusters jump to the ''solidlike'' phases, are higher than the bulk melting temperatures for Si, Ge, and Sn, which are 1685, 1210, and 505 K, respectively. For Sn, even the transition temperatures T_2, at which the Sn clusters transform into their ''ground-state'' phases, are higher than the Sn bulk melting temperature. In experiment it is found that the clusters Sn_n ($n \leqslant 50$) never melt or dissociate up to 600 K,[28] suggesting that Sn clusters may have melting temperatures higher than that of the bulk crystalline phase. As we have shown in Fig. 1, Sn, Ge, and Si clusters in small and medium size range do not resemble any fragment of the corresponding bulk systems. Thus it is not surprising that their ''melting'' temperatures are higher than the corresponding bulk ones because of the essential difference in structure.

For C_{13}, we performed three independent CP simulation runs by cooling the sample from 4500, 4000, and 3500 K, respectively. Even though the starting configurations were compact structures, the first and second annealings led to an open linear-chain structure while the third annealing yielded a monocyclic ring [shown in Fig. 8(a)], which is energetically much lower than that of the open chain. The animation of the first and second annealing simulations shows that above 3500 K the C atoms sometimes form a ring and sometimes an open-chain where the open-chain structure has much more probability than the ring structure. When the temperature continues to decrease the system is locked into the open-chain structure and no longer goes to the ring structure. This result suggests that above 3500 K the open-chain structure has larger entropy than the ring structure, and there also exists a quite large entropy barrier between these two kinds of structures. In the third annealing, an open chain structure never happens. A tadpole structure predominates above 3000 K, which is a monocyclic ring with a small linear chain attached to the ring.[29] In our simulation, the tadpole structure with 4 atoms in the chain [shown in Fig. 8(b)] has the most probability while the others with 3, 2, and 1 atoms in the chains are also found. A monocyclic ring structure appears below 3000 K and remains to the end of simulation, although large distortion, vibration, and rotation occur during the simulation. In the recent experiment of mobility measurements for Carbon cluster anions,[30] the tadpoles are recognized as the metastable isomers, which occurs in the early stages of Carbon cluster growth. Our simulation and the experiment are thus in an agreement.

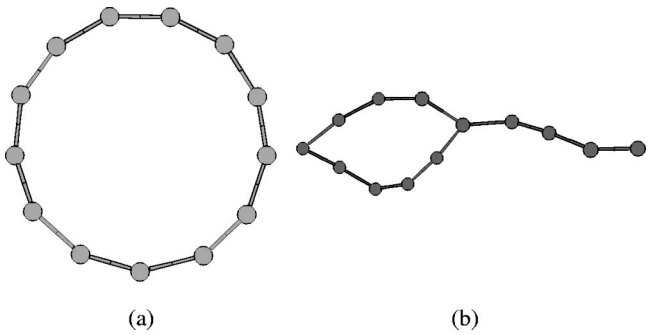

FIG. 8. C_{13}: (a) monocyclic ring as the ground structure; (b) tadpole structure with 4 atoms in the attached chain, which was found to have the most probability to appear in the simulated annealing when the temperature is above 3000 K, but less than 3500 K.

IV. CONCLUSION

We have demonstrated that CP *ab initio* MD simulations can be extended to medium-sized semiconductor clusters to study dynamical properties and ground structures of the clusters. Our simulation results show that C_{13} prefers a monocyclic ring structure, while Si, Ge, and Sn clusters have more compact geometries. These cluster structures are very different from any fragment of the corresponding bulk materials. New structures are found for Sn and Ge clusters from our simulations. By analyzing the trajectories of our simulations, we are able to identify the transition from the ''liquidlike'' phases to the ''solidlike'' phases, and the transitions among the different isomers during the cluster formation process.

ACKNOWLEDGMENTS

We thank Dr. Alexandre Shvartsburg and Professor Martin Jarrold for stimulating discussion. Ames Laboratory is operated for the U.S. Department of Energy by Iowa State University under Contract No. W-7405-Eng-82. This work was done on the T3E-900 parallel computer of National Energy Research Supercomputing Center (NERSC). Part of this work was made possible by the Scalable Computing Laboratory, which is funded by the Iowa State University and Ames Laboratory.

[1] K. Raghavachari and V. Logovinsky, Phys. Rev. Lett. **55**, 2853 (1985); K. Raghavachari and C.M. Rohlfing, J. Chem. Phys. **89**, 2219 (1988); C.M. Rohlfing and K. Raghavachari, Chem. Phys. Lett. **167**, 559 (1990).

[2] K. Raghavachari and J.S. Binkley, J. Chem. Phys. **87**, 2191 (1987); P. Ballone and P. Milani, Phys. Rev. B **42**, 3201 (1990); J. Bernholc and J.C. Philips, J. Chem. Phys. **85**, 2358 (1986); C.H. Xu, C.Z. Wang, C.T. Chan, and K.M. Ho, Phys. Rev. B **47**, 9878 (1993); R.O. Jones, J. Chem. Phys. **110**, 5189 (1999).

[3] W. Andreoni, D. Sharf, and P. Giannozzi, Chem. Phys. Lett. **173**, 449 (1990).

[4] P. Ballone, W. Andreoni, R. Car, and M. Parrinello, Phys. Rev. Lett. **60**, 271 (1988).

[5] I. Vasiliev, S. Öğüt, and J.R. Chelikowsky, Phys. Rev. Lett. **78**, 4805 (1997).

[6] Kai-Ming Ho, Alexandre A. Shvartsburg, Bicai Pan, Zhong-Yi Lu, Cai-Zhuang Wang, Jacob G. Wacker, James L. Fye, and Martin F. Jarrold, Nature (London) **392**, 582 (1998).

[7] P. Jackson, I.G. Dance, K.J. Fisher, G.D. Willett, and G.E. Gadd, Int. J. Mass Spectrom. Ion Processes **157**, 329 (1996).

[8] The consensus about the ground structure of C_{20} has not yet been fully reached. LDA calculation supports the fullerene structure as the ground state while GGA supports the ring structure. See the paper, E.J. Bylaska, P.R. Taylor, R. Kawai, and J.H. Weare, J. Phys. Chem. **100**, 6966 (1996).

[9] R. Car and M. Parrinello, Phys. Rev. Lett. **55**, 2471 (1985).

[10] For Si_n clusters, it had been done up to $n=18$. See the Ref. 6.

[11] P. Hohenberg and W. Kohn, Phys. Rev. **136**, B864 (1964); W. Kohn and L.J. Sham, Phys. Rev. **140**, A1135 (1965).

[12] O. Sugino and R. Car, Phys. Rev. Lett. **74**, 1823 (1995).

[13] Zhong-Yi Lu, Guido L. Chiarotti, S. Scandolo, and E. Tosatti (unpublished).

[14] N. Takeuchi, A. Selloni, and E. Tosatti, Phys. Rev. B **55**, 15 405 (1997); Phys. Rev. Lett. **72**, 2227 (1994).

[15] I. Stich, M. Parrinello, and J. M. Holender, Phys. Rev. Lett. **76**, 2077 (1996).

[16] N. Takeuchi and I. Garzón, Phys. Rev. B **50**, 8342 (1994).

[17] D.M. Ceperley and B.J. Alder, Phys. Rev. Lett. **45**, 566 (1980); J.P. Perdew and A. Zunger, Phys. Rev. B **23**, 5048 (1981).

[18] D.R. Hamann, M. Schlüter, and C. Chiang, Phys. Rev. Lett. **43**, 1494 (1979).

[19] L. Kleinman and D.M. Bylander, Phys. Rev. Lett. **48**, 1425 (1982).

[20] R. Stumpf, X. Gonze, and M. Scheffler (unpublished).

[21] F. Tassone, F. Mauri, and R. Car, Phys. Rev. B **50**, 10 561 (1994).

[22] P.E. Blöchl and M. Parrinello, Phys. Rev. B **45**, 9413 (1992).

[23] H. Bilz and W. Kress, *Phonon Dispersion Relations in Insulators* (Springer-Verlag, Berlin, 1979).

[24] Another similar simulated annealing but with the cooling rate 4 K per 100 MD steps only yielded a metastable structure.

[25] U. Röthlisberger, W. Andreoni, and P. Giannozzi, J. Chem. Phys. **96**, 1248 (1992).

[26] M.F. Jarrold and V.A. Constant, Phys. Rev. Lett. **67**, 2994 (1991).

[27] Alexandre A. Shvartsburg, Martin F. Jarrold, Bei Liu, Zhong-Yi Lu, Cai-Zhuang Wang, and Kai-Ming Ho, Phys. Rev. Lett. **81**, 4616 (1998).

[28] Alexandre A. Shvartsburg (private communication); Alexandre A. Shvartsburg and Martin F. Jarrold (unpublished).

[29] D.L. Strout, L.D. Book, J.M. Millam, C. Xu, and G.E. Scuseria, J. Phys. Chem. **98**, 8622 (1994); A.L. Aleksandrov, V.M. Bedanov, Y.N. Morokov, and V.A. Shveigert, J. Struct. Chem. **36**, 906 (1995).

[30] Ph. Dugourd, R.R. Hudgins, J.M. Tenenbaum, and M.F. Jarrold, Phys. Rev. Lett. **80**, 4197 (1998).

[31] The cohesive energies are computed by the Dmol package V950, Biosym Technologies, San Diego, CA, 1995, which uses a double numerical plus polarization basis and the Vosko-Wilk-Nusair type exchange-correlation potential. The calculation in the cohesive energies by CP MD and DMOL approaches yields a constant shift.